Advances in Aircraft and Spacecraft Science, *Vol. 4, No. 6 (2017) 613–637*
DOI: https://doi.org/10.12989/aas.2017.4.6.613

Damage detection through structural intensity and vibration based techniques

G. Petrone*, A. Carzana, F. Ricci and S. De Rosa

Department of Industrial Engineering, Aerospace Section, University Federico II, Via Claudio 21, 80125 Naples, Italy

(Received July 27, 2017, Revised July 30, 2017, Accepted July 31, 2017)

Abstract. The development systems for the Structural Health Monitoring has attracted considerable interest from several engineering fields during the last decades and more specifically in the aerospace one. In fact, the introduction of those systems could allow the transition of the maintenance strategy from a scheduled basis to a condition-based approach providing cost benefits for the companies. The research presented in this paper consists of a definition and next comparison of four methods applied to numerical measurements for the extraction of damage features. The first method is based on the determination of the Structural Intensity field at the on-resonance condition in order to acquire information about the dissipation of vibrational energy throughout the structure. The Damage Quantification Indicator and the Average Integrated Global Amplitude Criterion methods need the evaluation of the Frequency Response Function for a healthy plate and a damaged one. The main difference between these two parameters is their mathematical definition and therefore the accuracy of the scalar values provided as output. The fourth and last method is based on the Mode-shape Curvature, a FRF-based technique which requires the application of particular finite-difference schemes for the derivation of the curvature of the plate. All the methods have been assessed for several damage conditions (the shape, the extension and the intensity of the damage) on two test plates: an isotropic (steel) plate and a 4-plies composite plate.

Keywords: damage detection; structural intensity; curvature method

1. Introduction

Accumulation of damage among structure can cause severe structural failures. Development of an early damage detection method for structural failure is one of the most important keys in maintaining the integrity and safety of structures.

Many different damages can be modelled depending on the cause of the damage, on the sizes of the involved elements and on the material of the assessed structure.

In the work by Liu and Swaddiwudhipong (1997), damages derived by low-velocity impacts have been modeled through the definition of degenerated shell elements that have been deformed by the contact-impact (further study by El-Abbasi and Meguid (1998), Liu *et al.* (2004)). However, this

*Corresponding author, Ph.D., E-mail: giuseppe.petrone@unina.it

https://www.techno-press.org/?journal=aas&subpage=7 ISSN: 2287-528X(Print), 2287-5271(Online)

type of damage only shows the effect of the impact on the shape of the elements and then on the behaviour of the deformed structure, whereas none of the material properties have been modified by this damage modelling.

An improved modeling technique for damages has been developed recently, focusing on the assessment of nonlinear features of damages. The basic model of a nonlinear crack using finite elements is to have disconnected elements with collocated nodes, as used by Lee *et al.* (2006). This scheme, although easy to implement, can lead to non-physical conditions as the crack surfaces do not interact and structural elements may end up overlapping. Accordingly, this approach cannot take into account for contact friction or interaction forces between the crack surfaces. Therefore, this scheme should only be used when the physical crack or damage feature is actually behaving as disconnected elements with negligible interaction.

An improved model of a crack is the bilinear stiffness model assessed deeply by Hambric *et al.* (2012) (also by Al-Shudeifat and Butcher (2011) for cracked beams) which accounts for changes in stiffness at a node over time. As the stiffness between the surfaces changes depending on whether the crack is "open" or "closed", the stiffness alternates between two values assigned to the open and closed states. However also this method requires accurate contact modelling in order to obtain a realistic change of the dynamic behaviour of the plate due to the presence of the crack.

Many different methods for the detection of such a damage have arisen during the last decades, based on the determination of the change in structural response due to the reduction of material elastic properties. Structural intensity (SI) reveals the magnitude and direction of mechanical energy flow, or power flow, through a structure. Knowledge of SI fields is vital in the study of structure-borne noise as it reveals the sources and sinks of vibrational energy, as well as the dominant paths of energy flow, as functions of both space and frequency. The vibrational energy features can be very useful for general monitoring purposes and in particular can be of great importance for damage detection. The SI field determination is possible through the measurement of internal forces and displacement, hence it can be measured experimentally by using accelerometers for flexural wave propagation in beam and plate structures (first measurements were obtained by Noiseux (1970)).

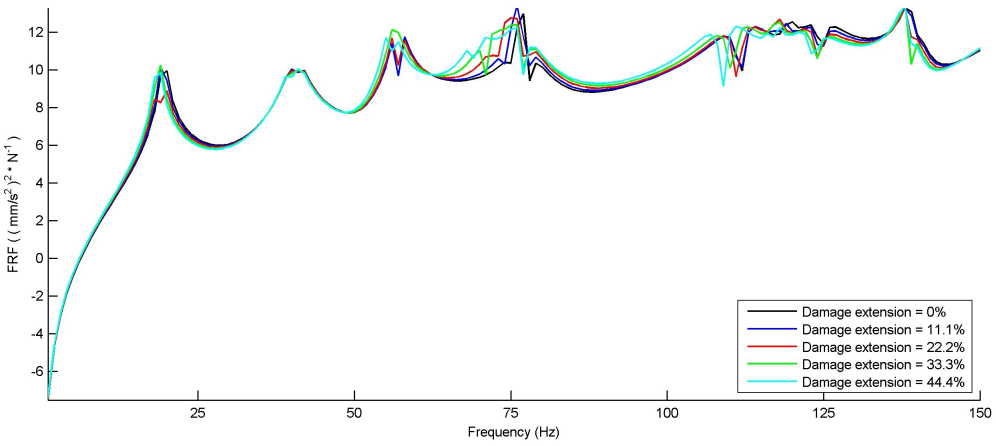

Fig. 1 FRF of a damaged plate

All the SI measurements methods require large numbers of sensors in order to obtain detailed power flow maps. To complement the experimental SI methods, numerical methods have been developed since they allow for mapping the intensity over the entire structures; this is particularly useful when experimental techniques are extremely limited or not possible. Moreover, benefits of numerical analysis include no equipment requirements or experimental loading and ease of adjusting loading and drive conditions. Numerical-based SI methods have also been developed primarily using finite element analysis (FEA), indeed it is cost-effective for low- to mid-frequency analysis and meshes are relatively easy to create and to analyse using commercial software packages. The SI field is able to show the mechanical energy paths in a clearer way whether the structure is assessed at on-resonance condition. Indeed if the forcing frequency is close to one of the natural frequencies, then the system will show a resonance response and hence greater vibrations. The onset of vibration waves is related to the mechanical energy flow, and this is the reason why the SI based methods seem to be the most valuable techniques for structure response analysis under resonance condition.

Similar considerations has led to the definition of other damage detection methods based on the evaluation of the frequency response function (FRF) under resonance condition. Unlike the SI based techniques, these methods require no modal analysis or other complex post-processing operations to obtain an estimate of relative structural health. As it is possible to see from Fig. 1, the FRF of a plate slightly changes with the increase of the damage extension, obtained reducing the mechanical properties of a given area. Hence it is possible to compare the frequency response of a damaged plate with the one of a healthy plate. It is easy to see that the higher distance between the curves is obtained at the natural frequencies, i.e., close to the resonance peaks, and therefore it has been demonstrated why the assessed FRF based techniques need the evaluation of the response function at on-resonance condition.

Although their ease of use, the damage detection methods based on the determination of the system response (squared acceleration of all nodes of the model) to a fixed excitation force are not able to track the position of the damaged area, but only its presence and extension. Therefore another FRF method has been applied in order to provide information about the position and intensity of the damage. The analysis of the mode shapes curvature makes possible to detect the crack location through the assessment of the change of the material properties, and in particular of the elastic modulus. The derivation of the curvature is possible through the application of various finite difference schemes to the nodes displacement value, hence yielding an accuracy of the method that depends on the density of the mesh.

Recently, two interesting papers appeared in literature, Jalali and Noohi (2018) and Guo and Xu (2018): they certified the active interests in engineering research field for such applications.

In this paper the background on structural intensity is given in Section 2 together with the detection methods to be investigated. Section 3 presents a summary of the numerical models and the results are in Section 4. Some concluding remarks in Section 5, close the work.

2. Theoretical background and models

2.1 Structural Intensity

The “vibration intensity”, or “structural intensity” (the denomination comes from the analogy with acoustic intensity), gives significant information about the strength and location of sources, sinks and

transmission paths of structure energy through the plotting of a vector map. The methods based on the analysis of the SI field hence provide relevant datas about the structure vibro-acoustic properties that can be used to better understand the behavior of the studied model (e.g. a plate). Although this technique is applicable to every type of vibration energy wave, most of the focus during the years has been put on the flow of flexural waves. Indeed this type of waves are the most relevant in order to analyse the energy radiation and dissipation of the structure.

The determination of the Power Flow or the Structural Intensity in simplified structures such as thin plates has been the focus of much work in recent years (Verheij (1980), Cuschieri (1987), Arruda and Mas (1996), Hambric (2009), Petrone *et al.* (2016)). The difference between all the methods developed by several authors during the last about 40 years is represented by the procedure for the input measurements. These measurements can be accelerations, displacements, rotational displacements, etc. The definition of *Instantaneous Power Flow* is due to Noiseux (1970), and represents an energy flux, a power rather than a flow intensity. For the case of a two dimensional structure such as a plate, it is possible to express the components of this vector in the direction *x* and *y* as follow

$$P_x(x,y) = Q_x\dot{w} - M_{xy}\dot{\theta}_x + M_x\dot{\theta}_y \tag{1a}$$

$$P_y(x,y) = Q_y\dot{w} - M_{xy}\dot{\theta}_y + M_x\dot{\theta}_x \tag{1b}$$

Typically, the *Time Average Power Flow* is more easily measurable and then of major interest with respect to the instantaneous power flow, hence the Eq. (1) can be easily modified in

$$P_x(x,y) = \langle Q_x\dot{w}\rangle_T - \left\langle M_{xy}\dot{\theta}_x\right\rangle_T + \left\langle M_x\dot{\theta}_y\right\rangle_T \tag{2a}$$

$$P_y(x,y) = \langle Q_y\dot{w}\rangle_T - \left\langle M_{xy}\dot{\theta}_y\right\rangle_T + \left\langle M_y\dot{\theta}_x\right\rangle_T \tag{2b}$$

where: Q_x and Q_y are respectively the shear forces in the x and y directions, M_x and M_y are the x and y directed bending moments, M_{xy} is the twisting moment, $\dot{w}$ is the normal velocity, $\dot{\theta}_x = \frac{\partial w}{\partial y}$ and $\dot{\theta}_y = \frac{\partial w}{\partial x}$ are the time rate of change of slope in the x and y directions, $\langle\,\rangle_T$ denotes the time average.

Few years after Noiseux' studies, Pavic (1976), proposed a novel concept for power flow in structures, called *Structural Surface Intensity*, or simply *Structural Intensity* (SI), no more based on measurement of forces and moments acting on the plate, but on the evaluation of internal normal and shear stress. If we consider that σ_x and σ_y are the surface normal stress components, τ_{xy} is the surface shear stress, $\dot{w}_x$ and $\dot{w}_y$ are the surface velocities, and $\langle\,\rangle_T$ denotes the time average, then the definition of SI components based on Pavic works can be expressed as follows

$$I_x = -\langle\sigma_x\dot{w}_x\rangle_T - \langle\tau_{xy}\dot{w}_y\rangle_T \tag{3a}$$

$$I_y = -\langle\sigma_y\dot{w}_y\rangle_T - \langle\tau_{xy}\dot{w}_x\rangle_T \tag{3b}$$

The determination of the internal forces-displacements or stress-strain at all the nodes of the model can be obtained through experimental or numerical methods. The experimental methods are based on the application of several linear and rotational accelerometers to the surface of the plate. Their accuracy is highly dependent on the number of measurements and on the specific finite difference

scheme applied. Moreover the experimental measurements show several errors due to the inaccuracy of the instruments and the attachment method. In numerical investigation, the acquisition of the forces and moments (Power Flow assessment), or the stresses and strains (Structural Intensity) are carried out by a FE model analysis, as shown by Gavric and Pavic (1993). The Eq. (3) can be generalized by considering the components of the SI in the i^{th} and j^{th} directions. Then by neglecting the effect of the shear stress, the SI component can be defined as follows

$$I_i = I_i(t) = -\sigma_{ij}(t)\dot{w}_{ij}(t) \qquad i,j = 1,2,3 \tag{4}$$

where $\sigma_{ij}(t)$ and $\dot{w}ij(t)$ are the stress and velocity in the j^{th}-direction at time t. It is possible to replace the velocities with the displacements by using the commonly adopted complex algebra and since the stresses and displacements are usually determined through an integration over the thickness, then the SI can be expressed as a power flow per unit width. The expression for the two components of the SI can be hence expressed as

$$I_x = -\frac{\omega}{2}\,\Im[N_x\tilde{u} + N_{xy}\tilde{v} + Q_x\tilde{w} + M_x\tilde{\theta}_y - M_{xy}\tilde{\theta}_x] \tag{5a}$$

$$I_y = -\frac{\omega}{2}\,\Im[N_y\tilde{v} + N_{xy}\tilde{u} + Q_y\tilde{w} - M_y\tilde{\theta}_x + M_{xy}\tilde{\theta}_y] \tag{5b}$$

where N_x and N_y are the complex axial forces, N_{xy} is the complex in-plane shear force, Q_x and Q_y are the complex transverse shear forces, M_x, M_y and M_{xy} are the complex bending moments, $\tilde{u}$, $\tilde{v}$ and $\tilde{w}$ are the complex conjugate of translational displacements, $\tilde{\theta}_x$, $\tilde{\theta}_y$ and $\tilde{\theta}_z$ are the complex conjugate of rotational displacement along *x*, *y* and *z* directions. $\Im$ denotes the imaginary part.

This method has become widely used because of its very low cost and its ease of execution, and also for its substantial reduction of experimental errors. In addiction to this, the coupling between a numerical and a non-contact method, for example a laser acquisition, may allow a very fast and accurate real-time control of plates and panels. On the other hand, great attention must be put on the choice of the FEM elements (e.g., beam, shell or plate elements) in order to obtain a good approximation of the experimental model.

Through finite element simulation, Lim *et al.* (2006) have shown that damage causes fundamental changes in the structural intensity fields of plates. In these analytical studies, changes in magnitude and phase angle of the intensity fields were observed in areas directly surrounding the crack. When a structure presents any type of crack damage, energy flow must divert around the crack, causing local changes in SI vector divergence. When determination of the Structural Surface Intensity over an entire structure is possible, it shows potential for use in damage localization and indication of damage severity. However when determination of the SI field over an entire structure is not possible or too difficult, classical FRF techniques can be used to show the presence of a damaged area.

2.2 The detection methods

The damage detection methods that will be here presented, are based on the assessment of the Frequency Response Function defined as the ratio between the squared acceleration of the nodes (output) and the fixed excitation force (input). Hence these methods can be applied to directly measured frequency response data, providing a real-time monitoring of the structural health.

A widely used metric for the damage detection in a mode shape is the *Modal Assurance Criteria* (MAC). The MAC is used to find correlation characteristics between two given matrices: the first

matrix consists of the first N mode shapes of an healthy plate, and the second consists of the same N mode shapes in a damaged plate. The MAC is represented by a [NxN] matrix that provides information of the correlation between the two sets of different mode shapes, and therefore where a lack of correlation denotes the presence of a damage. Since the MAC has proven helpful with applications in damage detection through use of mode shape data it has been expanded into the frequency domain. A direct expansion of the MAC into the frequency domain yields the *Response Vector Assurance Criterion* (RVAC) and the *Global Amplitude Criterion* (GAC).

In the MAC, each mode shape in a system reference state is compared to each mode shape in a current state. This provides a resultant matrix where the diagonal terms represent comparison between same mode shapes. Hence being the RVAC a direct expansion of the MAC into the frequency domain, it is only applied along the equivalent of the diagonal of the MAC matrix. This means that only similar frequencies (same modes) are compared between the damaged and undamaged states. The RVAC, is defined as

$$RVAC(\omega) = \frac{\left|\sum_{i=1}^{n} \alpha_i^d(\omega)\alpha_i^*(\omega)\right|^2}{\sum_{i=1}^{n}\left[\alpha_i^d(\omega)\alpha_i^{d*}(\omega)\right]\sum_{i=1}^{n}\left[\alpha_i(\omega)\alpha_i^*(\omega)\right]} \tag{6}$$

where $\alpha(\omega)$ is the healthy FRF at frequency ω, $\alpha^d(\omega)$ is the damaged FRF at frequency ω, and $*$ denotes the complex conjugate.

The input for the RVAC at a given frequency is a set of two vectors. One vector contains the magnitude of the FRF at each degree of freedom for a reference case, and the other vector contains equivalent quantities for a damaged or current case. The output of the RVAC for a single frequency is a scalar quantity between 0 and 1, where a RVAC value of 1 corresponds to perfect correlation and 0 corresponds to no correlation. The RVAC can be applied at any number of frequencies (in this study just the first 9 modes have been considered) such that the total output of the RVAC is a vector containing one scalar value for each frequency evaluated.

Another frequency response-based metric that determines correlation between a baseline and current system state is the GAC. Similar to the RVAC, the GAC is based on a 0 to 1 scale where 1 corresponds to perfect correlation and 0 corresponds to no correlation.

The GAC takes the form defined as

$$GAC(\omega) = \frac{1}{n}\sum_{i=1}^{n} \frac{2\left|\alpha_i^{d*}(\omega)\alpha_i^d(\omega)\right|}{\left[\alpha_i^*(\omega)\alpha_i(\omega)\right] + \left[\alpha_i^{d*}(\omega)\alpha_i^d(\omega)\right]} \tag{7}$$

The GAC uses the same input as the RVAC (two vectors containing frequency response data for a healthy and current structural state), and the output is a 1 x n vector where n represents the number of frequencies at which the reference and current states are compared. While on the surface the GAC may look very similar to the RVAC, the mathematical derivation of these two parameters are slightly different. Nevertheless, the output of the GAC is a vector with a length equal to the number of frequencies studied, which is comparable to the RVAC.

It is not always helpful to have to interpret data in vector form. In reality, it is much simpler to handle a single number that may become an indicator of damage when it crosses a certain threshold. As a result, the *Damage Quantification Indicator* (DRQ) and the *Average Integrated Global Amplitude Criterion* (AIGAC) were developed. The DRQ converts the RVAC vector output into a scalar

quantity by averaging all of the values of the RVAC. In practice, the DRQ can be assigned a critical threshold. If the DRQ falls below this value, critical structural damage has been achieved, and repairs to the structure have to be undertaken. The DRQ is defined as

$$DRQ = \frac{1}{N_\omega} \sum_{k=1}^{N_\omega} RVAC(\omega_k) \tag{8}$$

where N_ω represents the total number of frequencies for which the RVAC is calculated. The DRQ shows potential in damage detection applications because it is an FRF based damage detection method where the output is a single number. This implies that it can be used in real-time systems where a "damaged" or "undamaged" indicator can be used. One shortcoming of the DRQ is that it cannot be used as a damage localizer as it is a global damage detection technique. This is simply a consequence of the DRQ's scalar output. The AIGAC has the same definition of the DRQ, but it represents the average value of the GAC vector. The AIGAC is defined as

$$AIGAC = \frac{1}{N_\omega} \sum_{k=1}^{N_\omega} GAC(\omega_k) \tag{9}$$

2.3 Mode shape curvature method

The *Mode Shape Curvature method* has been used here then to provide complementary information with respect to the previously cited FRF methods. To implement this method, measured nodes displacement value at all experimental grid points are isolated at specific frequencies (plate natural frequencies). By isolating the transfer functions at a single frequency, an operational "mode shape" at the frequency of interest is obtained. The presence of a damage is the cause for a reduction of elastic modulus into an area, but this has an effect on the curvature of a plate through the definition of the flexural stiffness

$$M_x = -D \left(\frac{\partial^2 w}{\partial x^2} + \nu \frac{\partial^2 w}{\partial y^2} \right) \tag{10a}$$

$$M_y = -D \left(\frac{\partial^2 w}{\partial y^2} + \nu \frac{\partial^2 w}{\partial x^2} \right) \tag{10b}$$

where

$$D = \frac{Eh^3}{12(1-\nu^2)} \qquad \text{with: } h = \text{plate thickness} \tag{11}$$

The curvature of the plate, i.e., the 2^{nd}-order derivative of the displacement in the in-plane directions, can be therefore studied in order to acquire information about the presence of a damage. The approximated derivatives shown in Eq. (10) have been obtained through the application of a *central finite difference scheme* (curvature in border elements has been derived through $forward$ and $backward$ schemes instead).

A further study has been performed in order to determine the most accurate definition of curvature for the damage detection. Two types of curvature have been defined and assessed

$$\textit{Mean Curvature} : \kappa_{mean} = \frac{1}{2}\left(\frac{\partial^2 w}{\partial x^2} + \frac{\partial^2 w}{\partial y^2}\right) \tag{12a}$$

$$\textit{Gauss Curvature} : \kappa_{Gauss} = \frac{\partial^2 w}{\partial x^2} \cdot \frac{\partial^2 w}{\partial y^2} \tag{12b}$$

The evaluation of the curvature values of the elements can be derived by averaging the curvature values of the four corner nodes of each square element. The elements curvature has to be found for all the natural frequencies included in an arbitrary range (in this study the first nine have been taken), and then it is possible to calculate for each element the residual value through the formula expressed in Eq. (13) for the i^{th} element

$$R_i = \sum_{n=1}^{N_f} \left|\kappa_{i,n}^d - \kappa_{i,n}^h\right| \tag{13}$$

where N_f is the number of natural frequencies considered, D and H denote that the curvature is related to the damaged or the non-damaged (healthy) plate respectively.

The plotting of the residuals is used to show clearly the effect of the presence of a damaged area on the modes shape and hence on the modes curvature.

2.4 Summary

The four detection methods to be tested inside this work are thus

- RVAC
- GAC
- DRQ
- AIGAC

Given the nature of the AIGAC calculation, it has the same inherent advantages and disadvantages in damage detection applications as the DRQ. The trait that separates the DRQ from the AIGAC is the formulation of the GAC. The AIGAC is an averaged integration of the GAC, a lesser used and lesser known formulation than the MAC. Since the GAC is not as well known in damage detection applications as the MAC, the true potential of the AIGAC in damage detection is unknown.

Both the DRQ and the AIGAC can be used as global damage detection techniques, and hence are not able to determine the position and shape of the damaged area or crack.

3. Numerical models

3.1 Damage

In this paper, the damage studied has been modeled as a fatigue crack that involves just some elements of the plate (Simmermacher *et al.* (2012)).

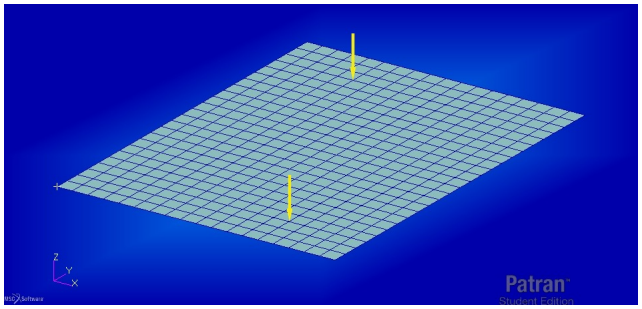

Fig. 2 Plate model

For a finite element model with N elements, the elastic moduli for the elements can be denotes as

$$E = \{E_1, E_2, \ldots, E_i, E_{i+1}, \ldots, E_{i+n}, \ldots, E_{N-1}, E_N\} \tag{14}$$

The damage is represented by a change in the flexural rigidity or stiffness of the plate, which, in turn, is reflected by a reduction in the elastic modulus of the damaged elements. If the model contains n damaged elements, their elastic moduli $\{E_{i+1}, \ldots, E_{i+j}, \ldots, E_{i+n}\}$ are replaced by

$$E_d = \{k_{i+1}E_{i+1}, \ldots, k_{i+j}E_{i+j}, \ldots, k_{i+n}E_{i+n}\} \tag{15}$$

where $k_{i+j}, j = 1, \ldots, n$, denotes the reduction factor (lower than 1) for the $(i + j)$th damaged element.

3.2 Plates

The assessed structure is a rectangular plate with size 1080×1440 mm, Fig. 2, and is modelled through a mesh of 18×24 four nodes elements. The plate is simply supported on all edges and is subjected to a nodal excitation force applied at position *P*(300 mm, 1260 mm). The applied force has a magnitude of $1N$ and a frequency of 20 Hz, indeed it is possible to assess through a normal mode analysis that 20 Hz is a value close to the first natural frequency. The mechanical energy introduced into the plate is dissipated by a viscous damper attached at the position *Q*(780 mm,180 mm), defined by a damping coefficient $\zeta = 0.5$. Both the force and damper locations are represented in Fig. 2 by yellow vertical arrows indicating the selected node.

Two different materials have been chosen for the analysis performed in this dissertation in order to provide a complete set of information about the applicability of these damage detection methods to different structures. The first assessed plate has a thickness of 6 mm and is made of isotropic steel having the properties shown in Table 1.

Table 1 Isotropic steel properties

E	G	ν	ρ
205.6 GPa	79.15 GPa	0.3	7800 kg/m^3

Table 2 Orthotropic lamina properties

E_x	E_y	G_{xy}	G_{xz}	G_{yz}	ν_{xy}	ν_{xz}	ν_{yz}	ρ
175.1 GPa	6.7 GPa	4.1 GPa	2.056 GPa	4.1 GPa	0.254	0.469	0.469	1520 kg/m^3

The second study case is about a composite plate made of four orthotropic laminas stacked together and having the following orientations: $\pm 90^\circ / 0^\circ / 0^\circ / \pm 90^\circ$. The single lamina is a 2 mm thick composite ply made of graphite fibers and epoxy resin matrix, therefore it has been given the material properties exhibited in Table 2.

Note that the *x*-direction is parallel to the shorter side of the plate, and the *y*-direction is then perpendicular and directed as the long edge. The structural damping parameter η has been set equal to 0.007 in both study cases. This value is consistent with the measurements made on sample metallic and composite structures. A higher structural damping would produce a greater dissipation of the mechanical energy flow along its path, and therefore a decrease of the damper effectiveness.

3.3 Modal information

Numerical simulations were conducted, in terms of modal analysis and frequency response function, using the commercial finite element solver Nx/Nastran, focusing on the low frequency region. The first natural frequencies of both investigated panels, under simply-supported boundary condition, are reported in Table 3.

In order to simulate a structural fault, the Young modulus of some elements of the isotropic plate model, has been reduced progressively: the results of [10, 30, 50, 70]% variations have been obtained. All analysis have been carried out by starting from a damaged area of 120 mm and extending this up to 480 mm. Results obtained by these analysis are represented in Table 4. It can be noticed that the frequencies shift methods are not very sensitive to bending stiffness variation. As a matter of fact, with a big reduction of the Young modulus (70%) in a region, the variation of the value of the modal frequencies is too small to be detected and hence a different approach is needed.

Table 3 First natural frequencies of Isotropic and orthotropic panels

Mode hline number	Steel plate Natural frequency $[Hz]$	Graphite-epoxy plate Natural frequency $[Hz]$
1	19.73	31.92
2	40.94	36.88
3	57.60	48.80
4	76.32	69.01
5	78.26	97.21
6	112.78	123.75
7	120.72	126.70
8	125.86	132.88

Table 4 First natural frequencies of isotropic plate for different damage intensity and dimension

Damage extension		E modulus reduction			
		10%	30%	50%	70%
$120mm$	Mode 1 [Hz]	19.72	19.71	19.64	19.66
	Mode 2 [Hz]	40.94	40.94	40.93	40.93
	Mode 3 [Hz]	57.60	57.60	57.59	57.59
	Mode 4 [Hz]	76.29	76.22	75.91	76.02
$240mm$	Mode 1 [Hz]	19.71	19.64	19.56	19.43
	Mode 2 [Hz]	40.93	40.93	40.92	40.91
	Mode 3 [Hz]	57.59	57.55	57.51	57.45
	Mode 4 [Hz]	76.23	75.91	75.47	74.73
$360mm$	Mode 1 [Hz]	19.69	19.61	19.49	19.30
	Mode 2 [Hz]	40.93	40.92	40.91	40.88
	Mode 3 [Hz]	57.56	57.45	57.34	57.18
	Mode 4 [Hz]	76.15	75.72	75.06	73.92
$480mm$	Mode 1 [Hz]	19.68	19.58	19.43	19.18
	Mode 2 [Hz]	40.93	40.91	40.88	40.85
	Mode 3 [Hz]	57.52	57.33	57.09	56.77
	Mode 4 [Hz]	76.11	75.57	74.74	73.25

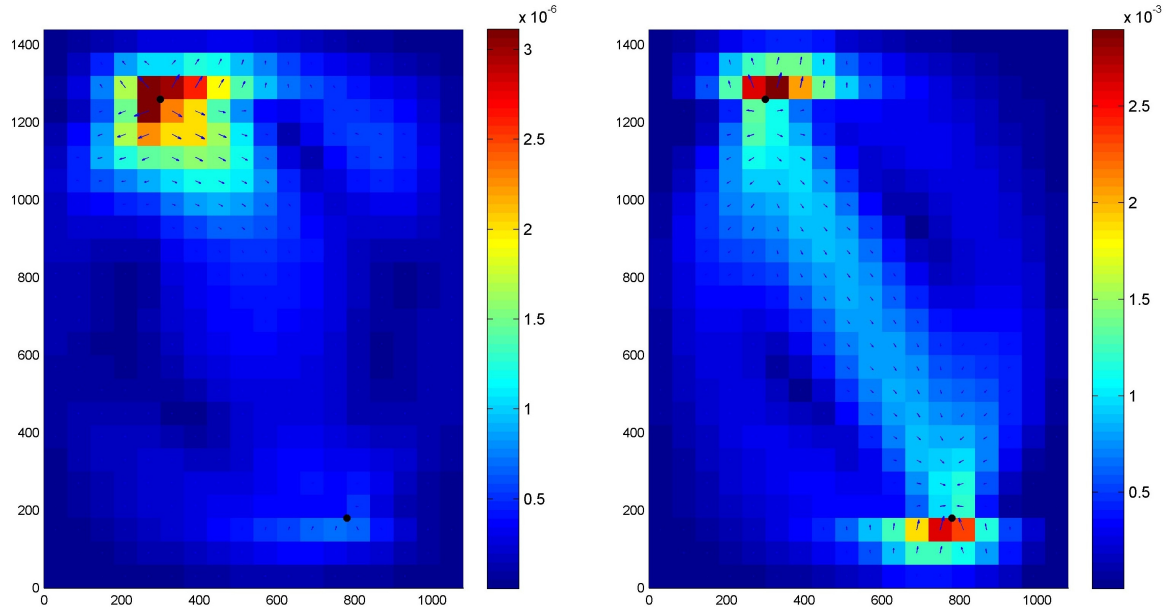

(a) Healthy Composite Plate: Horizontal fibres (b) Healthy Composite Plate: Vertical fibres

Fig. 3 Graphite/Epoxy Composite Plate, SI method for different fibers orientation

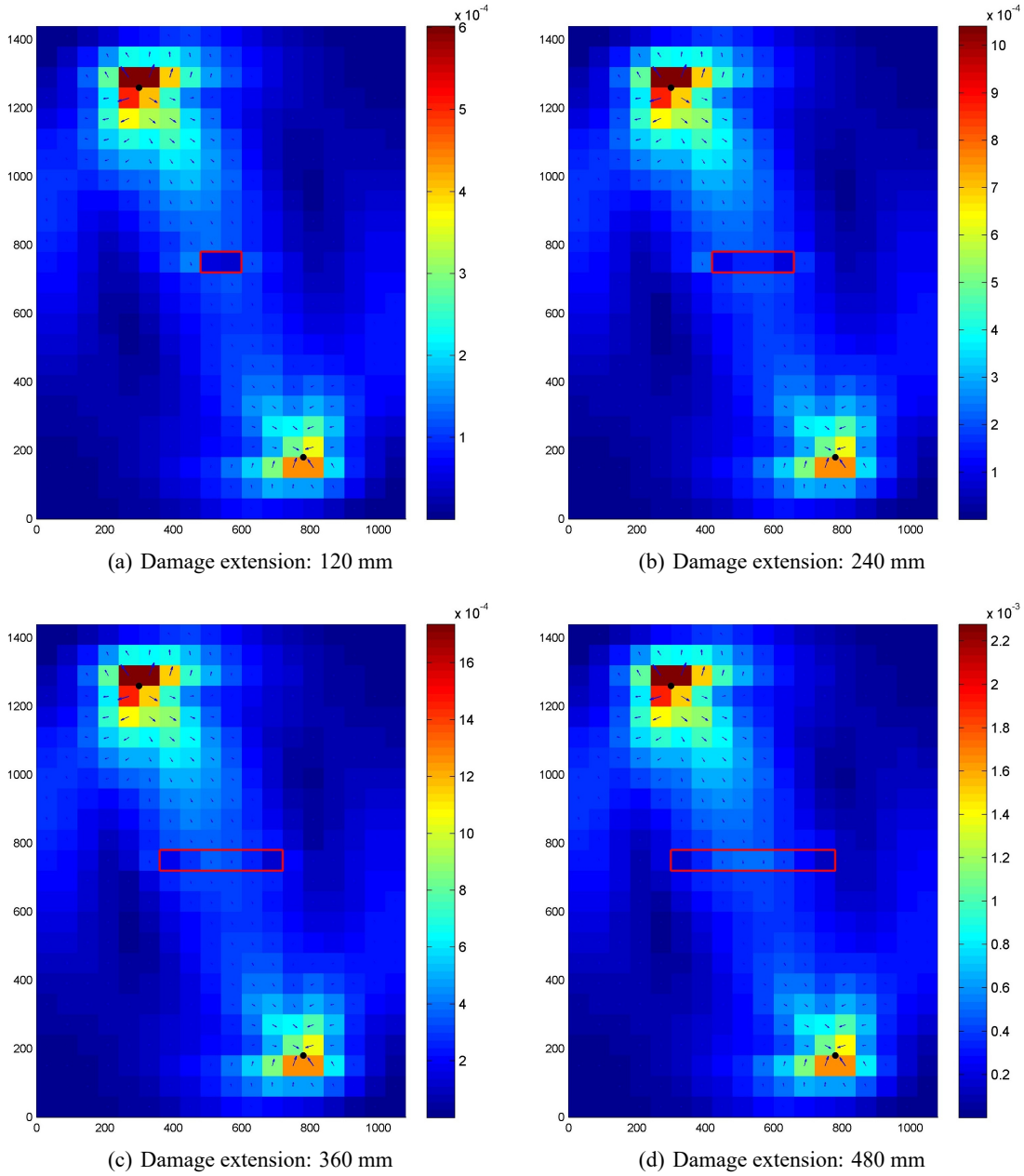

(a) Damage extension: 120 mm

(b) Damage extension: 240 mm

(c) Damage extension: 360 mm

(d) Damage extension: 480 mm

Fig. 4 Steel plate, SI method for different crack extension

4. Damage detection

4.1 Isotropic plate

The Structural Intensity based method has been applied to the isotropic steel plate in order to detect the presence of a damage, and in particular to assess its size and intensity.

Five cases have been examined corresponding to 5 different lengths of the central damaged area:

- healthy plate;
- 120 mm (11.1% of plate width);
- 240 mm (22.2% of plate width);
- 360 mm (33.3% of plate width);
- 480 mm (44.4% of plate width);

In this first study the damage intensity has been fixed to 70%; this means that the elastic properties (E and G) of the elements belonging to the damaged area have been decreased of the 70% of their original value. As expected, the SI field of the damaged plates represented in Fig. 4 shows the path of mechanical energy that flows from the source of vibrations, i.e., the external force position at the top-left corner, to the viscous damper at the bottom-right corner of the plate.

The reduction of elastic stiffness due to the presence of a damage has a deep effect on the divergence of the SI flow, hence producing a change in the vectors phase and magnitude for the elements belonging to the damaged region or close to it. Moreover it can be seen through the scale on the right side of the images that the presence of a crack has a relevant effect also on the global magnitude of SI, i.e., on the average value of $|SI|$. A further analysis on the steel plate SI field has been developed in order to provide information about the effect of the increase of damage intensity on the flow of vibrational energy. In this study case the damage extension has been fixed to a length of 240 mm, i.e., about the 22.2% of the plate width, while the damage intensity varies in a range that goes from 30% to 90%.

Even in this case, as can be seen from the Fig. 5, the damage intensity has an effect on the global magnitude of structural intensity that hence is reflected by a variation of the scale on the right of the pictures. The increase of damage intensity yields to a significant deepening of the "hole" representing the crack, and therefore a more accentuate deviation of the SI flow.

The SI field of the plate has been plotted by using a specific MatLab function (*imagesc*) that automatically defines the scale represented by the color bar beside the figures. Therefore it is easy to see that different crack conditions (damage extension and intensity) determine a particular magnitude color scale, then making difficult to compare the figures in order to make proper conclusions. This problem has been solved through the definition of a new parameter that could make the comparison between different crack conditions easier, and then representing a more effective damage detection method.

A "reference" value of the SI magnitude has been derived for each element of the horizontal band passing through the damaged area. Hence this band has a width equal to the plate size in the x-direction, i.e., 1080 mm, and a height of 60 mm. The reference value of SI magnitude for the i^{th} element (ΔSI_i) has been derived through the Eq. (16), with $i = 1, 2, ...N_b$ and N_b that is the number of elements belonging to the selected horizontal band.

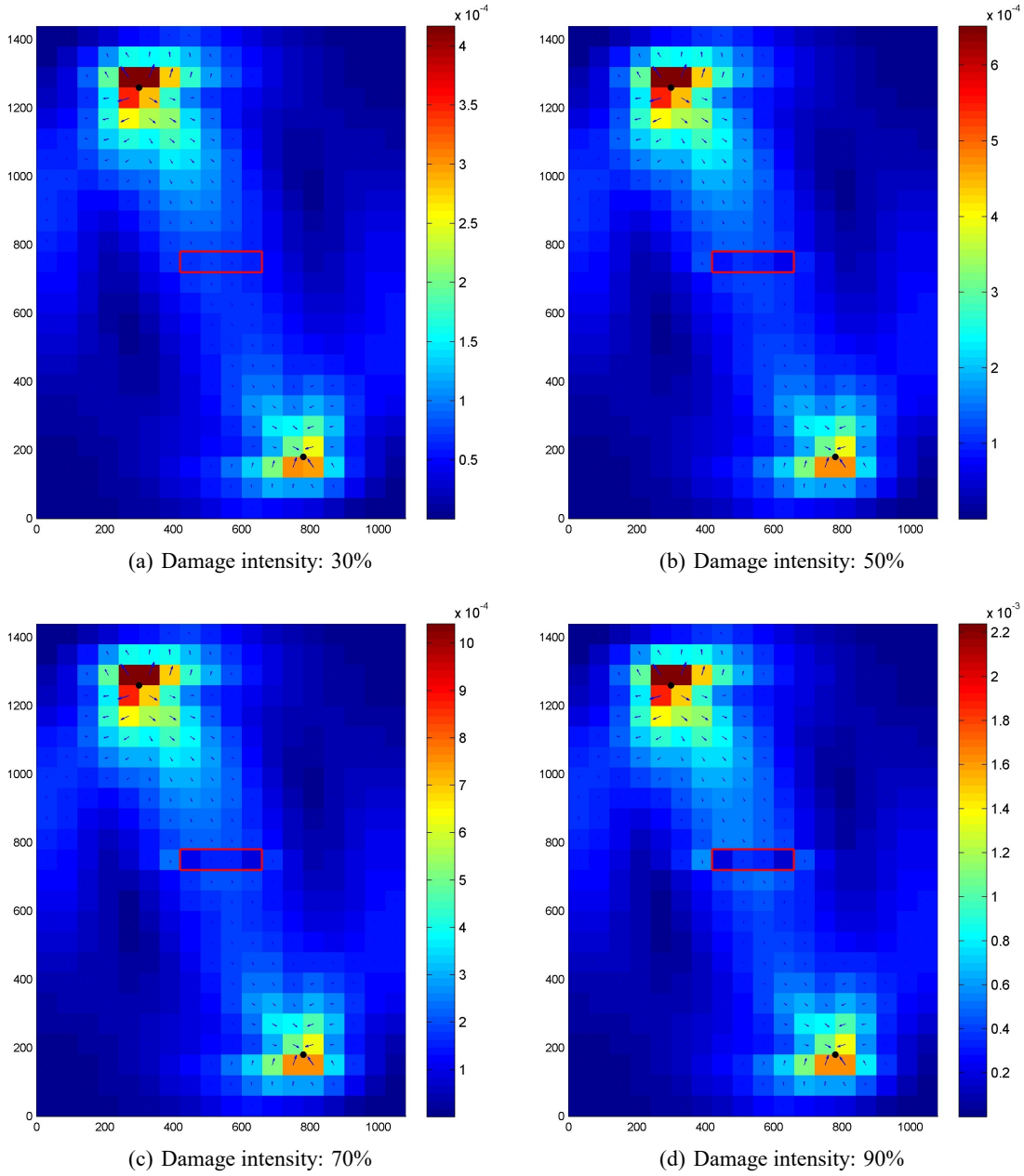

(a) Damage intensity: 30%

(b) Damage intensity: 50%

(c) Damage intensity: 70%

(d) Damage intensity: 90%

Fig. 5 Steel plate, SI method for increasing damage intensity

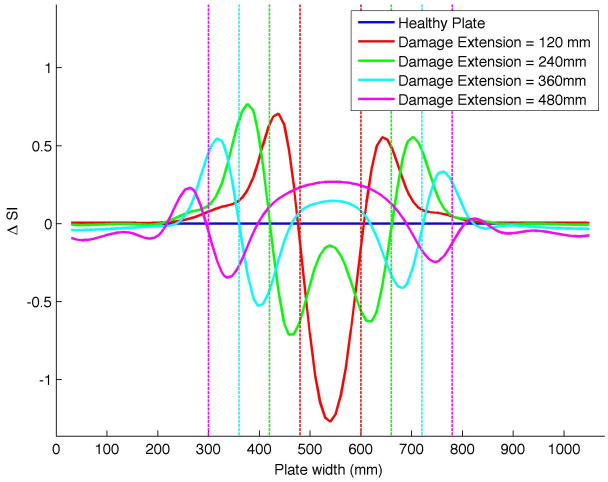

Fig. 6 ”Reference” Structural Intensity for central band elements: effect of crack extension

$$\Delta SI_i = \frac{M_i^D}{M_{av}^D} - \frac{M_i^H}{M_{av}^H} \tag{16}$$

where M_i^D is the SI magnitude of the i^{th} element in the damaged plate, M_{av}^D is the SI average magnitude of the i^{th} element in the damaged plate, M_i^H is the SI magnitude of the i^{th} element in the healthy plate, and M_{av}^H is the SI average magnitude of the i^{th} element in the healthy plate.

This modified definition for the SI can be applied in order to derive a more accurate SI based damage detection method. The SI flow diverts from its original path (the healthy plate case) then yielding an increase of the magnitude in the elements directly surrounding the crack. This is reflected in Fig. 6 as positive peaks of ΔSI outside the range delimited by the two vertical dotted lines (the

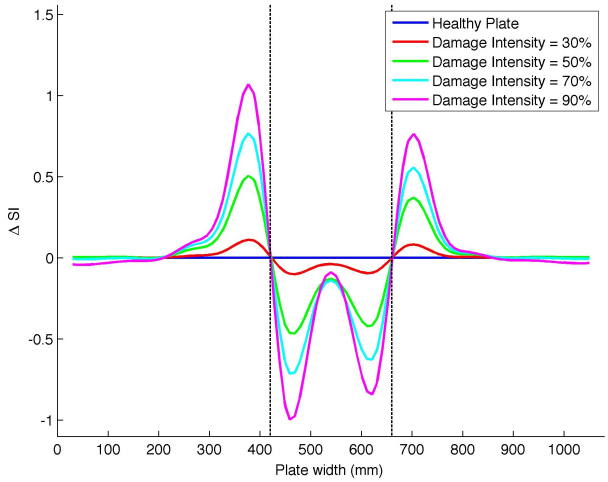

Fig. 7 ”Reference” Structural Intensity for central band elements: effect of damage intensity

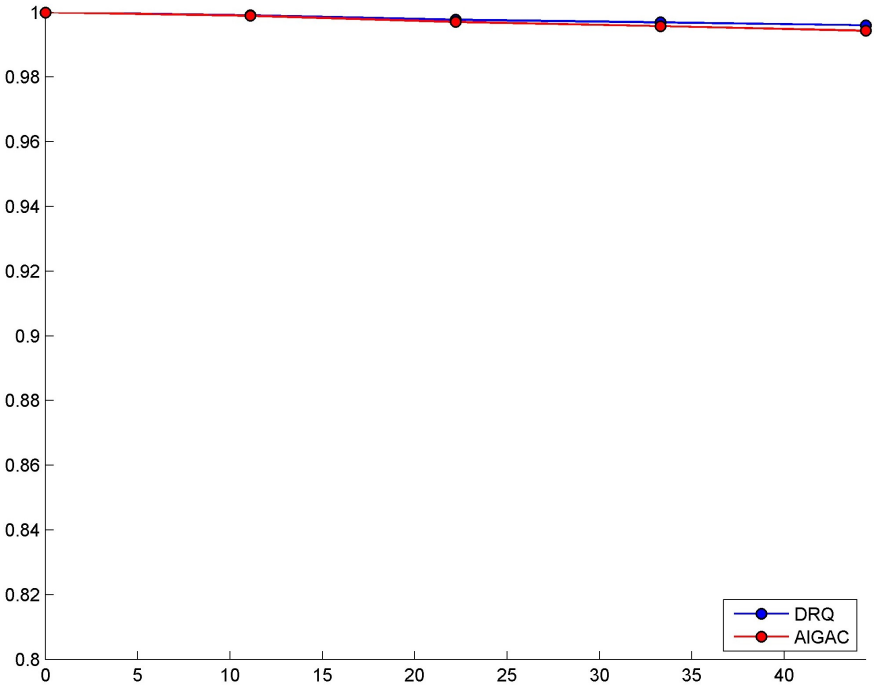

(a) Damage Intensity $< 50\%$

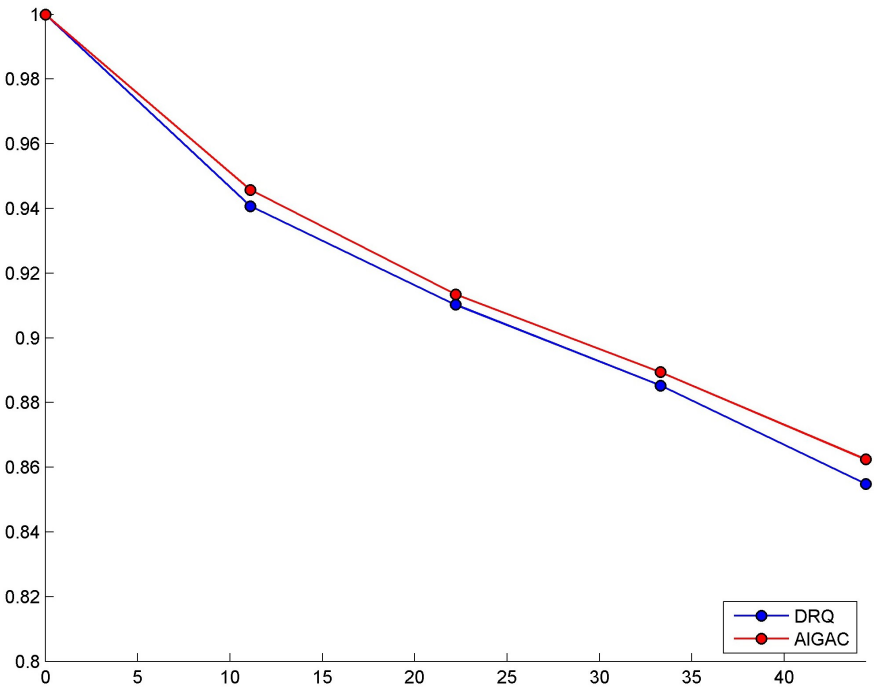

(b) Damage Intensity $\geq 50\%$

Fig. 8 DRQ and AIGAC plot for isotropic steel plate

crack position). On the opposite, the damaged elements, i.e., the ones that are inside the cited range, show a drop of ΔSI that is more intense with the decrease of the crack extension.

It can be noted that the crack tip location corresponds to the external points where there occurs the value of ΔSI goes from positive to negative, or the opposite. When the damage extension is high, the internal elements of the crack, i.e., far from the crack tips, show an increase in magnitude due to the fact that the flow is not able to provide an adequate deviation, and hence is forced to pass through the crack width.

The study of the ΔSI for several damage intensities shows that through this method it is possible to detect even very soft damages, as it is exhibited in Fig. 7. Indeed for very small cracks the targeting of the damaged region is eased with respect to the case of great crack extension because all the damaged elements exhibit a negative value of ΔSI whereas all the other external elements show positive values.

Despite their accuracy, the SI based damage detection methods are not so common because of the great effort required for the measurements. Therefore, FRF based techniques are preferable in some cases. The assessment of DRQ and AIGAC has been carried out for the same damage conditions already studied before, i.e., the healthy plate case and four cases for an increasing crack extension. By looking at Fig. 8 it is possible to make some considerations about these two parameters used to investigate the presence of a damaged area inside the plate.

The sensitivity of these methods has been obtained, indeed both DRQ and AIGAC do not seem to be able to detect any damage if the intensity is too low, e.g. less than the 50%. In this case their values is about constant and equal to 1 for every extension of the crack, and this means that the FRFs of the healthy and damaged plate are exactly the same, i.e., no significant damage is observed.

All the numerical simulations performed with damage intensity values above or equal to 50% (i.e., 90%, 70% and 50%) have yielded exactly the same graph for DRQ and AIGAC, hence this method is not able to determine the intensity of a damage, but just its existence and the crack length. Both the DRQ and the AIGAC decrease with the increase of the crack extension, and this suggests a damage maintenance criterion based on the definition of an arbitrary threshold (a sample value could be 0.92) that indicates whether a crack maintenance intervention needs to be applied.

The DRQ curve is placed in a slightly lower position than the AIGAC curve, therefore showing to be a more conservative approach and hence preferable with respect to the AIGAC.

The last FRF based damage detection technique that has been applied to the isotropic steel plate is the mode shape curvature method. This is based on the derivation of the curvature along the x and y directions from the measurement of the nodal displacements. Hence the input FRF vectors are different with respect to the ones required for the application of the DRQ and AIGAC methods.

The difference of the mathematical definition between the mean and Gaussian curvature yields a change in the damage detection power of the curvature method (Fig. 9). The assessed plate shows a central damage with an extension of 240 mm and a very low intensity, i.e., a reduction of elastic stiffness equal to the 30% of the value corresponding to a healthy plate.

The curvature method shows to be ineffective when the damage intensity is too low, indeed in this case both the mean and the Gaussian curvature do not highlight clearly the shape of the crack. It is possible to observe that the Gaussian curvature is less accurate than the mean curvature because it leads to a wrong prediction of the damage position (a feasible crack location might be at the top-right and bottom-left corners, based on Fig. 9(b)). However the accuracy of the mean curvature

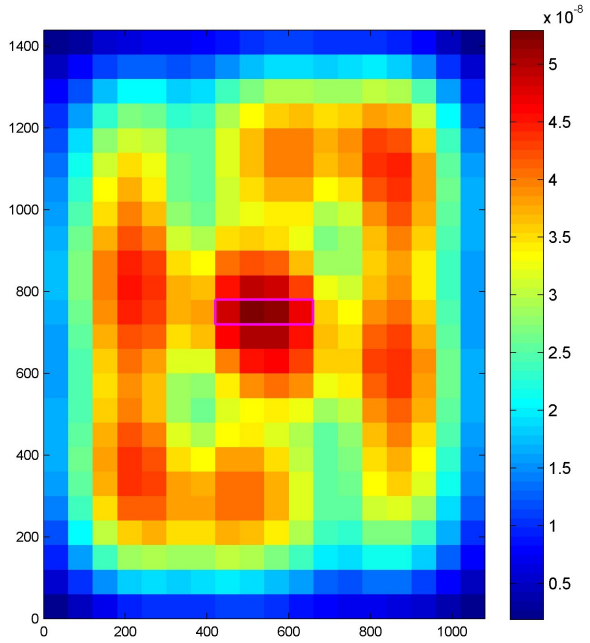

(a) Mean Curvature

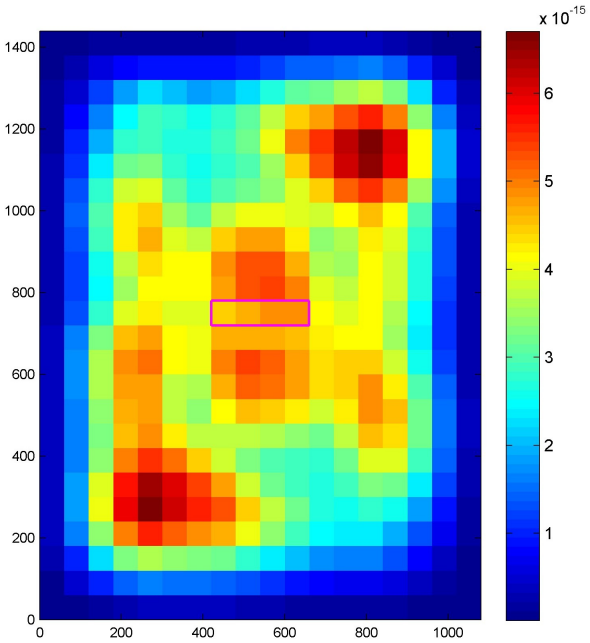

(b) Gauss Curvature

Fig. 9 Curvature method: damage extension of 240 mm and intensity of 30%

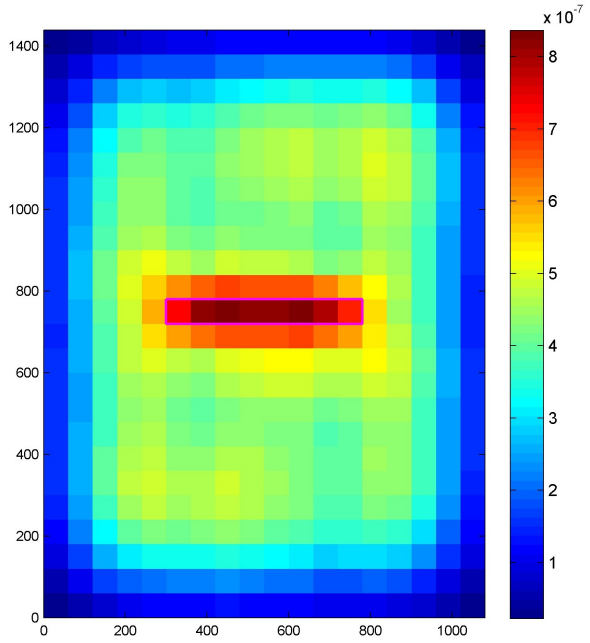

(a) Mean Curvature

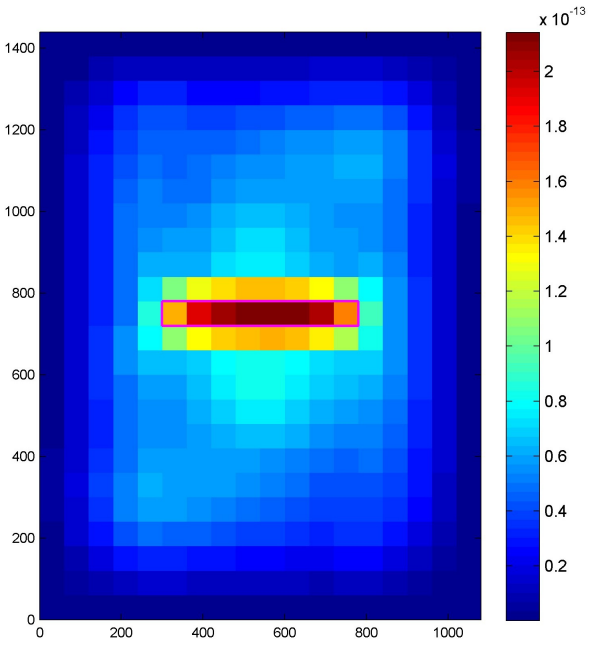

(b) Gauss Curvature

Fig. 10 Curvature method: damage extension of 480 mm and intensity of 70%

drastically decreases with the increase of the crack extension, making this method useless for the damage detection.

Opposite considerations can be made when the same methods are applied to a plate that presents a deeper and larger crack, e.g., 70% of damage intensity and 480 mm of crack extension, such as the one shown in Fig. 10. Obviously an intense damage is more easily recognized by any damage detection technique, however it is possible to note that the Gauss Curvature method is more accurate than the Mean Curvature method. Indeed it is possible to track the right contour of the crack only by looking at Fig. 10(b)), whereas Fig. 10(a)) provides a lower gradient between the damaged and the undamaged area of the plate.

The different mathematical definition of the mean and Gaussian curvature makes impossible to compare the magnitude of the residuals deriving from the applied method (the first is of the order of 10^{-7} whereas the second is of the order of 10^{-13}), but it determines a complementarity of the information provided. In conclusion it is essential to assess both the curvature residuals field in order to detect the presence of a crack in all damage conditions.

4.2 Composite plate

The study of an isotropic steel plate has provided relevant information about the power of the SI and FRF based methods for damage detection. However the application of the same methods to a composite plate can be used to make also some considerations on the role that the single plies have on the transmission of vibrational energy throughout the plate.

The high level of anisotropy of the graphite/epoxy composite lamina produce a significant change in the power flow path with respect to the case of an isotropic (e.g., steel) plate. Indeed the mechanical energy is more easily transmitted through materials featuring high values of the elastic modulus (this is also the reason why a damage that is modelled as a region with a lower elastic stiffness yields a hole into the SI field). This means that the SI field completely changes with the change of the fibres orientation, and in particular the SI flow vectors are longer (i.e., higher magnitude) when the fibres have a direction that is about parallel to the dominant direction of the flow.

The comparison between a steel plate and two composite (Graphite/Epoxy) plates featuring orthogonal fibers is shown in Fig. 3. It can be easily seen how the application of vertical fibres to the composite plate is the choice that produces the greatest transmission of energy throughout the plate and hence the highest SI magnitude. On the opposite the choice of horizontally directed fibres strongly reduces the flow between the force and the damper, therefore decreasing the effectiveness of the viscous damper. The global magnitude shown by this last case is of the order of 10^{-6}, about one thousand times smaller than the SI magnitude of the plate with horizontal fibers, and even a hundred times smaller than the magnitude of the steel plate (see Figs. 4 or 5 as reference).

From the reported data and presented models, it is clear that a damage applied to the plies that are more involved in the SI transmission will be then detected with a greater accuracy with respect to damages applied to *less important* plies. The composite plate analysed here (and earlier presented) has been modelled with the external lamina parallel to the plate long edge and the internal lamina in the orthogonal direction, therefore it may be predicted that the damages applied to the external lamina should be more easily detectable. This result have be obtained through the assessment of the SI field for all crack conditions (Fig. 11). The comparison between the vibrational energy holes provided by different cracks leads to the determination of the most severe damage, i.e., the one applied to the

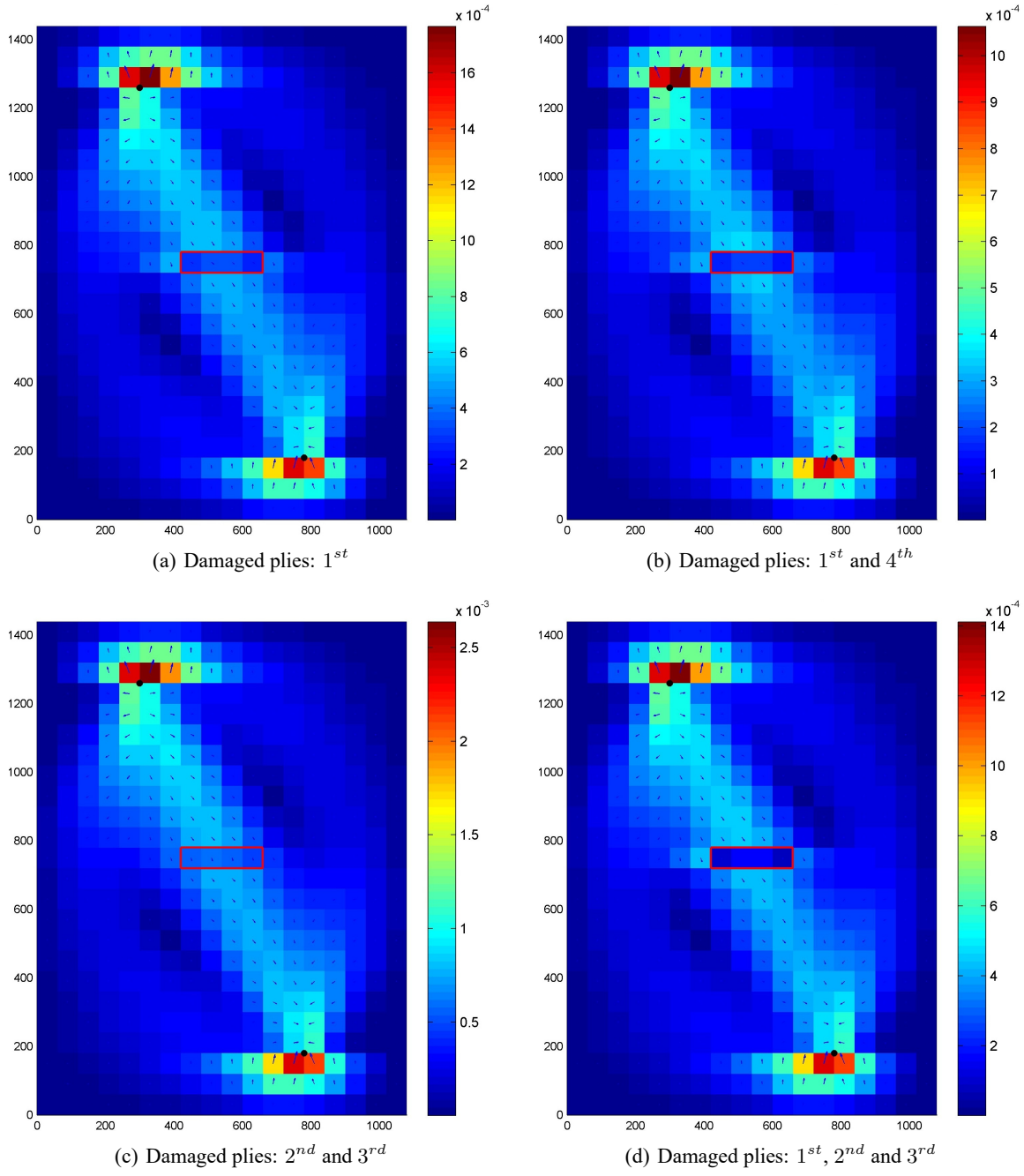

(a) Damaged plies: 1^{st}

(b) Damaged plies: 1^{st} and 4^{th}

(c) Damaged plies: 2^{nd} and 3^{rd}

(d) Damaged plies: 1^{st}, 2^{nd} and 3^{rd}

Fig. 11 Composite Plate, SI method for different damaged plies

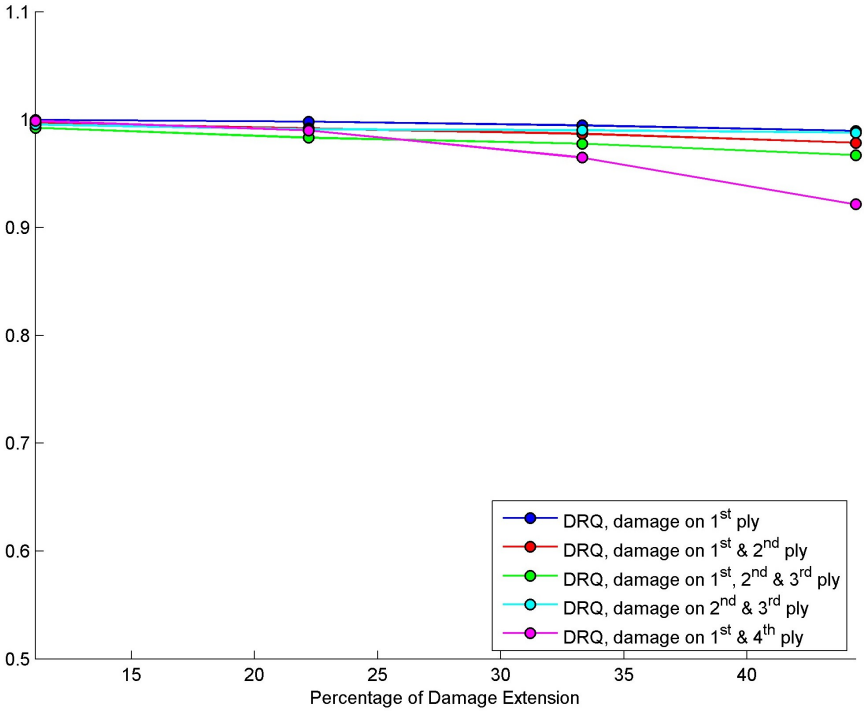

(a) DRQ plot

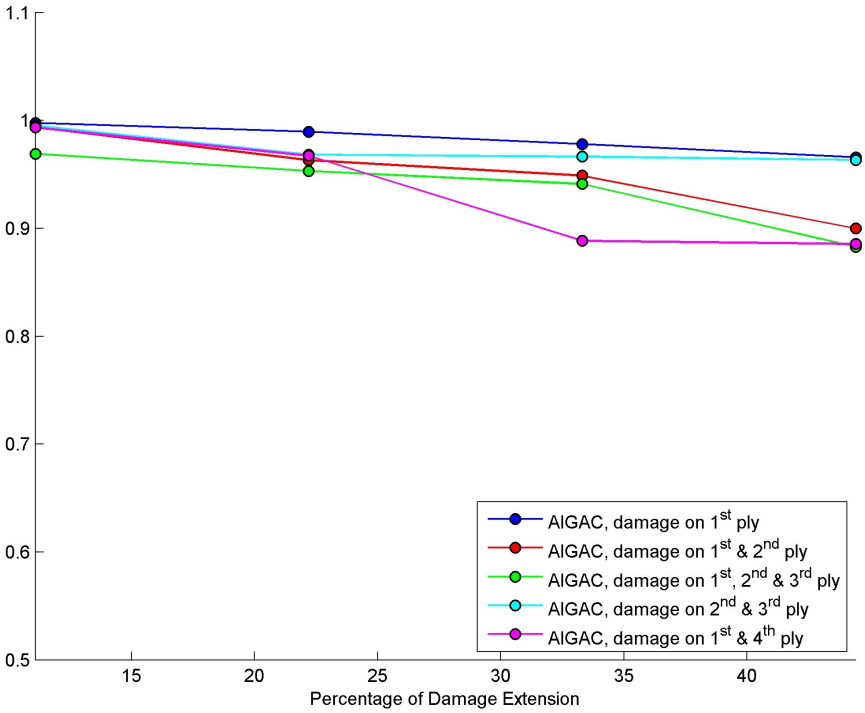

(b) AIGAC plot

Fig. 12 DRQ and AIGAC plot for a 4-plies composite plate

external plies as assumed before. However the global magnitude of the SI field that is highlighted by the color scale on the right of the pictures, significantly varies with the change of the crack position (the highest element SI magnitude goes from about $11 \cdot 10^{-4}$ to $2.5 \cdot 10^{-3}$), therefore a more accurate method needs to be applied in order to make it possible a comparison between the several cases.

The graphs shown in Fig. 12 make possible a deeper understanding of what it has been exposed previously. The study of the DRQ and AIGAC plot obtained through the application of FRF based methods, show that the plies fibres orientation has a great effect not only on the SI field, but on the FRF too. The damage has been applied to different plies in order to investigate their 'importance" for damage detection, and it has been found that the external plies (i.e., the 1^{st} and the 4^{th}) are more useful for this purpose. Indeed when the damage is applied to just 2 plies, i.e., we are assuming a crack of the same intensity and volume, it is easy to see that both the DRQ and AIGAC curves decrease with a higher gradient for that case with respect to the opposite condition of crack placed in the 2^{nd} and the 3^{rd} plies.

Once again the DRQ proves to be a more accurate method than the AIGAC method, indeed the curves in Fig. 12(a) exhibit a more constant slope with respect to the curves of Fig. 12(b). Moreover the AIGAC curve for the case of a damage applied to the 1^{st}, 2^{nd} and 3^{rd} plies (green line) shows a too low value for small crack extension (11.1%) due to numerical errors that are implicit in this method.

The damage intensity has been set to a value of 90%, indeed also for the study of a composite plate both the FRF methods have shown a sensitivity that prevents the detection for too soft damages (below 50% of intensity). Obviously the chosen model for damages does not take into account the interaction between near cracks, i.e., cracks applied to adjacent plies, hence assuming that each damaged volume is independent yields an underestimation of the intensity of a crack and its effect on the transmission of vibrational energy.

5. Conclusions

All numerical investigations that have been made in this work had the purpose of acquiring information about the behaviour of the dynamic response of a rectangular cracked plate. Several studies have been performed in order to assess the effects due to the variation of the crack extension and intensity, material parameters and fibres orientation with respect to the power flow direction. The use of FRF techniques such as the DRQ and the AIGAC has shown that the detection of an heavy damage can be obtained through the comparison with a scalar threshold that does not have to be trespassed. This limit is specific for the analysed structure, and moreover this method does have a sensitivity that prevents the detection of not very intense damages. Anyway, the ease of use of this techniques and the associated results encourage further investigations on the potentiality that have been shown through this work. In particular the DRQ has proven to be a much more reliable tool for damage detection than the AIGAC.

The localization of the damage has been obtained through the analysis of the SI field and through the study of the Curvature (Mean and Gaussian) of the plate. These two methods have proven to be both valid but characterised by different sensitivities to the damage extension and intensity. The study of the SI flow has led to the conclusion that the reduction of elastic modulus in the damaged area yields a hole in the SI field that can be easily observed. Once found the location of the damaged

area, the crack features can be then derived through an assessment of the ΔSI magnitude of only some selected plate elements. On the other hand the Curvature method has proven to be helpful on a wide range of damage conditions, and provide accurate indication of the crack location. Globally the FRF Curvature Method seems to be easier and more accurate than the SI based method.

In the last part of this paper, the study of the damages in a composite plate have shown important results, indeed it has been demonstrated that the damage applied to single plies is detectable by the FRF techniques that hence can clearly show which is the worst damage that a composite can withstand without falling below the expressed threshold.

References

Liu, Z.S. and Swaddiwudhipong, S. (1997), "Response of plate and shell structures due to low velocity impact", *J. Eng. Mech.*, **123**(12), 1230-1237.

Shepherd, M.R., Conlon, S.C., Semperlotti, F. and Hambric, S.A. (2012), "Structural intensity modeling and simulations for damage detection", *J. Vibr. Acoust.*, **134**(5), 051004.

Lee, H.P., Lim, S.P. and Khun, M.S. (2006), "Diversion of energy flow near crack tips of a vibrating plate using the structural intensity techniques", *J. Sound Vibr.*, **296**(3), 602-622.

Noiseux, D.U. (1970), "Measurement of power flow in uniform beams and plates", *J. Acoust. Soc. Am.*, **47**(1B), 238-247.

Pavic, G. (1976), "Measurement of structure borne wave intensity", *J. Sound Vibr.*, **49**(2), 221-230.

Lim, S.P., Lee, H.P. and Khun, M.S. (2006), "Diversion of energy flow near crack tips of a vibrating plate using the structural intensity technique", *J. Sound Vibr.*, **296**(3), 602-622.

El-Abbasi, N. and Meguid, S.A. (1998), "Large deformation analysis of contact in degenerate shell elements", *J. Numer. Meth. Eng.*, **43**(6), 1127-1141.

Liu, Z.S., Lee, H.P. and Lu, C. (2004), "Structural intensity study of plates under low-velocity impact", *J. Imp. Eng.*, **31**(8), 957-975.

Al-Shudeifat, M.A. and Butcher, E.A. (2011), "On the dynamics of a beam with switching crack and damaged boundaries", *J. Vibr. Contr.*, **19**(1), 30-46.

Simmermacher, T., Cogan, S., Horta, L.G. and Barthorpe, R. (2012), *Topics in Model Validation and Uncertainty Quantification*, Springer.

Verheij, J. (1980), "Cross-spectral density methods for measuring structure-borne power flow on beams and pipes", *J. Sound Vibr.*, **70**(1), 133-138.

Cuschieri, J. (1987), "Power flow as a complement to statistical energy analysis and finite element analysis", *Stat. Energy Analy.*

Arruda, J.R.F. and Mas, P. (1996), "Predicting and measuring flexural power flow in plates", *Proceedings of the SPIE the International Society for Optical Engineering*.

Hambric, S.A. (2009), "Power flow and mechanical intensity calculations in structural finite element analysis", *J. Vibr. Acoust.*, **112**(4), 542-549.

Petrone, G., De Vendittis, M., De Rosa, S. and Franco, F. (2016), "Numerical and experimental investigations on structural intensity in plates", *Compos. Struct.*, **140** 94-105.

Gavric, L. and Pavic, G. (1993), "A finite element method for computation of structural intensity by the normal mode approach", *J. Sound Vibr.*, **164**(1), 29-43.

Jalali, H. and Noohi, F. (2018), "A modal-energy based equivalent lumped model for open cracks", *Mech. Syst.*

Sign. Proc., **98**, 50-62.

Guo, T. and Xu, Z. (2018), "Data fusion of multi-scale representations for structural damage detection", *Mech. Syst. Sign. Proc.* **98**, 1020–1033.

EC